Astron. Astrophys. 339, 183–186 (1998)

ASTRONOMY AND ASTROPHYSICS

The mm-to-submm continuum spectra of W 3(OH) and K 3-50A

H.-P. Reuter[1] **and C. Kramer**[2]

[1] Max-Planck-Institut für Radioastronomie, Auf dem Hügel 69, D-53151 Bonn, Germany
[2] 1. Physikalisches Institut, Universität zu Köln, Zülpicher Strasse 77, D-50937 Köln, Germany

Received 3 June 1998 / Accepted 26 June 1998

Abstract. We present a model for the integrated flux density of W 3(OH) and K 3–50A allowing these sources to be used as reliable secondary calibrators between 80 and 800 GHz. Using new narrow-band continuum measurements between 86 − 245 GHz with the 30m telescope and reasonable assumptions about the source sizes, we construct continuum spectra from the mm-to-submm range which are in very good agreement with previously published data. With the fit parameters given in this paper, observers at any single-dish telescope will be able to calculate the expected flux densities of the two sources at any given aperture and frequency.

Key words: (ISM:) H II regions – ISM: individual objects: K 3-50A – ISM: individual objects: W 3(OH) – radio continuum: ISM

Table 1. Source positions

Source	α(1950)	δ(1950)
W 3(OH)	02 23 16.5	61 38 57.0
K 3–50A	19 59 51.1	33 24 19.4

Table 2. Source extents

Source	90 GHz	245 GHz[a]	384 GHz[b]
W 3(OH)	$\sim 6''$[c]	$14\times8''$ (p.a.=61°)	$14\farcs2 \times 10\farcs2$
K 3–50A	$\sim 2''$[d]	$11\times10''$ (p.a.=65°)	$10\farcs6 \times 5\farcs5$

[a] This paper
[b] Sandell 1994; source size is given in $\alpha \times \delta$
[c] Wink et al. 1994, including the H_2O maser source
[d] Howard et al. 1997

1. Introduction

The atmospheric extinction of radio waves, which is negligible in the meter-to-centimeter range, becomes significant at wavelengths short of 7 mm. The attenuation of the signal is highly weather dependent, especially close to atmospheric absorption lines of water and oxygen. A proper calibration of mm-wave measurements thus requires a proper knowledge about the atmospheric opacity, which is usually done by measuring the atmospheric emission relative to the emission from a cold and a warm load. Including information about atmospheric parameters, the application of an atmospheric model allows the determination of the water wapour content and hence the optical depth can be derived.

Even if the calibration procedure appears to work properly, independent cross-checks of the temperature scale are necessary in order to check the system set–up, e.g. the determination of the sideband ratios and the receiver temperatures. For spectral line observations, catalogues with calibrated reference spectra exist (e.g. Mauersberger et al. 1989) whereas continuum calibration checks are done by cross-scans on planets.

Only few planets can be used as reliable primary calibrators: Venus and Mecury show strong phase-dependent flux variations and the flux of Saturn is affected by the viewing angle of its rings. Uranus and Neptune are relatively weak and currently at low declinations which (at sites in the northern hemisphere) introduces an additional uncertainty. The disk temperature of Jupiter is stable but its disk is resolved by large single-dish mm/submm–telescopes, like the IRAM–30m telescope and the JCMT, and thus requires a complex deconvolution of the observed temperature profile which introduces additional errors into the calibration procedure. Mars appears to be the only planet which is mostly small enough not to be resolved by mm-wave telescopes and whose (frequency-dependent) disk temperature is well determined and stable. Proper continuum calibration checks are therefore restricted to a few hours per day when Mars is at sufficiently high elevations. In order to provide a set of reliable calibrators which are distributed more uniformly over the sky, we have undertaken sensitive narrowband (500 MHz) continuum measurements in the frequency range 86–245 GHz of the galactic HII–regions W 3(OH) and K 3–50A. Moreover, we present broadband (60 GHz) maps of the 1.2 mm dust continuum emission of these sources which provide information of the source sizes and their morphology.

Send offprint requests to: H.-P. Reuter, MPIfR, Bonn

Table 3. List of measured flux densities

Date	ν [GHz]	Flux density [Jy] W 3(OH)	K 3–50A
1994.207	87.0		6.17±0.22
	131.0		6.21±0.32
	221.0		8.40±0.96
1994.347	87.7	4.09±0.45	6.39±0.30
	142.0	4.42±0.20	6.74±0.63
1994.470	111.0	3.99±0.13	6.14±0.30
	142.0	4.01±0.14	
	223.0	5.37±0.30	6.03±0.90
1994.513	89.1	4.37±0.44	6.70±0.50
1994.600	87.7	3.98±0.18	6.46±0.25
	142.0	4.19±0.63	6.13±0.39
1994.634	87.7	3.88±0.25	6.19±0.26
	142.0	4.24±0.25	6.36±0.70
	219.0	6.24±1.00	6.75±1.30
1994.647	87.7	3.75±0.13	6.30±0.23
	142.0	4.50±0.36	6.20±0.42
	229.0	6.96±0.90	6.49±0.90
1994.772	109.8	3.78±0.24	
	145.0	4.61±0.35	
1994.865	87.7	3.84±0.15	
	142.0	4.31±0.11	
	221.0	6.73±0.96	
1994.879	87.7	3.63±0.15	5.94±0.28
	151.0	4.49±0.48	5.98±0.50
	233.0	6.60±0.73	6.74±0.70
1994.956	90.0	3.89±0.08	
	151.0	4.32±0.15	
	233.0	6.16±0.20	

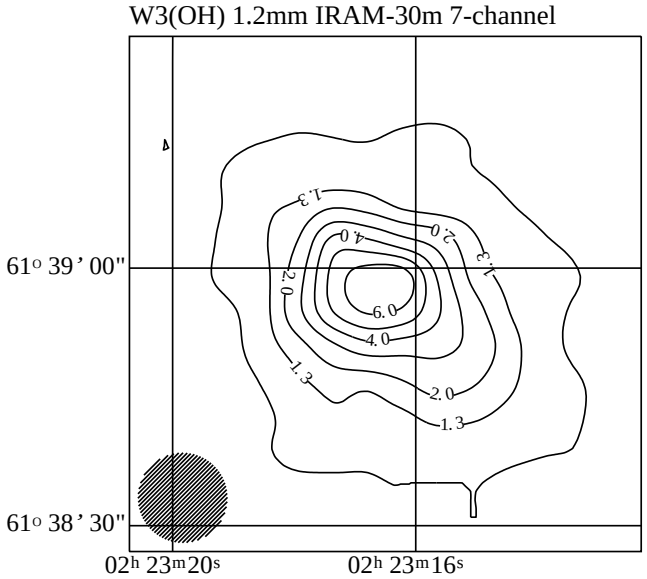

Fig. 1. Broadband 1.2 mm dust continuum map of W 3(OH) observed with the IRAM 7-channel bolometer array. Contour levels are: −0.65, 0.65, 1.3, 2, 3, 4, 5, 6 Jy/beam.

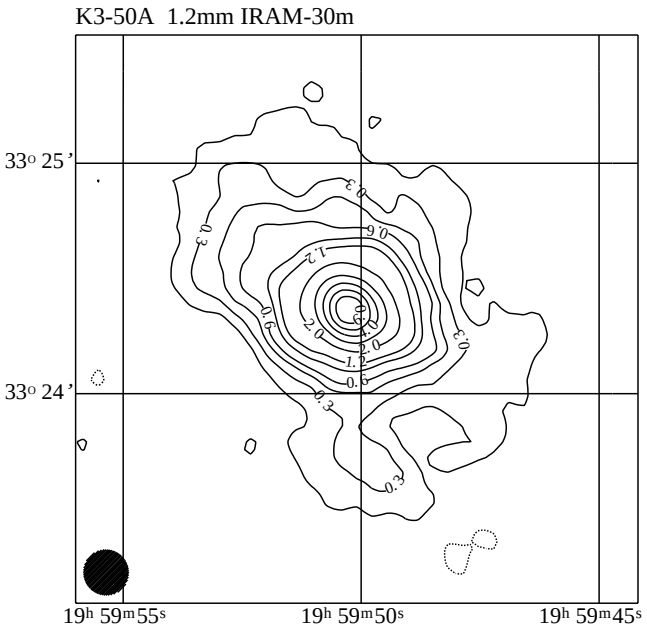

Fig. 2. Broadband 1.2 mm map of K 3–50A. Contour levels are: −0.15, 0.15, 0.3, 0.45, 0.6, 0.9, 1.2, 1.6, 2, 3, 4, 5, 6 Jy/beam The North-Eastern extension is K 3–50B (e.g. Salter et al. 1989)

2. Observations and calibration

The observations were done with the 30 m telescope under good atmospheric conditions. The maximum water vapour content during the observing runs was $\lesssim$5 mm. We used Mars as primary calibrator and cross–scans on Mars and on the HII–regions were mostly repeated at different hour angles allowing a check of the system stability. We assume brightness temperatures for Mars of 207, 210 and 213 K at 90, 150 and 227 GHz, respectively (Ulich 1981, Griffin et al. 1986) and we estimate the accuracy of the Mars flux determination to be less than five percent. The observations were done from May 1994 until mid-December 1994; during this time the disk of mars had an extent of $\lesssim 9''$ so that it was not resolved even with the smallest beamsize of $\approx 11''$ at 233 GHz.

Data acquisition and data reduction were done according to the procedure described by Reuter et al. (1997).

Gain–elevation corrections according to the curves shown by Wild (1995) were applied to the data. However, as the selected observations were done at intermediate elevations, these corrections usually did not exceed 5% in the 1 mm wave band where the gain dependence is strongest. Finally, for every observing session, a calibration factor was derived from the Mars scans and the measured antenna temperatures were converted into flux densities.

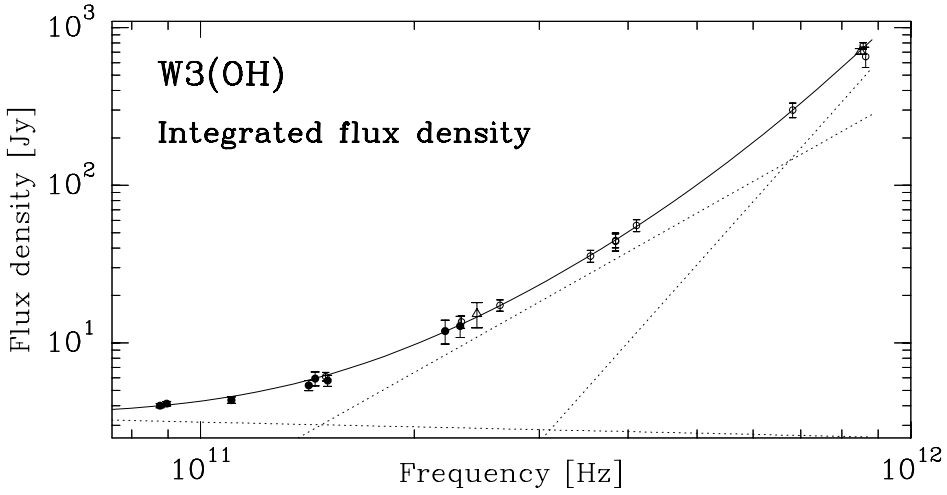

Fig. 3. The mm-to-submm continuum spectrum of the HII Region W 3(OH). The filled points are binned data listed in Table 3. Open circles are measurements by Sandell (1994) and the open triangles are data points from Altenhoff et al. (1994) at 250 GHz and from Chini et al. (1986) at 850 GHz. All the data have been multiplied following Eq. (1) and the procedure described in the text. The solid line is the fit to the observed points after Eq. (2) and the dotted lines are the contributions from one free-free and two dust components. The parameters of the fit are given in Table 4

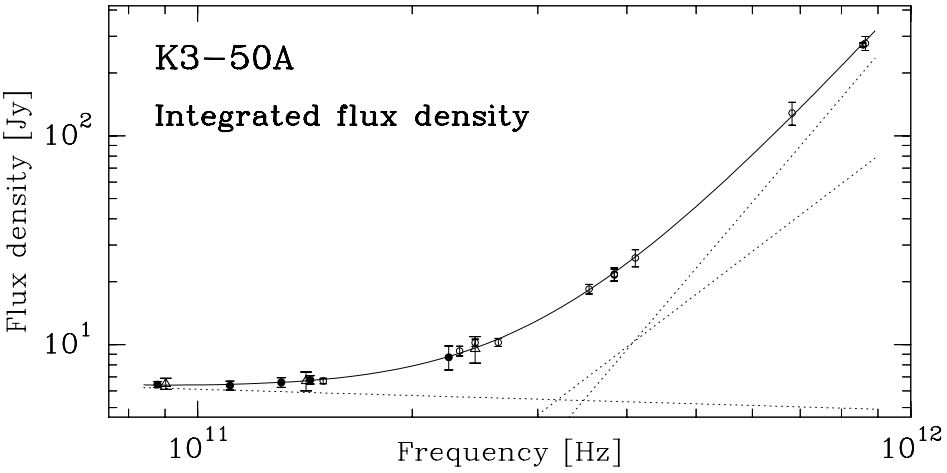

Fig. 4. The mm-to-submm continuum spectrum of K 3-50A. The symbols are the same as in Fig. 3.

3. Data from the submm–range

For a comparison with data from other telescopes, we have to convert measured peak flux densities to integrated fluxes for each source which requires knowledge of the source sizes. The size of the thermal Bremsstrahlung source is determined by interferometric observations at short cm–wavelengths. This value was used as an approximation for frequencies below 100 GHz where the contribution from dust emission is small. At $\nu \gtrsim 300$ GHz, dust emission dominates the integrated spectrum and we used the extent of the dust for the determination of total fluxes. In Table 2 we give the extent of the sources at different frequencies. The integrated flux densities were calculated by assuming both a gaussian shape of the sources and a linear increase of the source sizes with frequency. A constant source size was assumed above that frequency at which the dust emission clearly dominates the continuum spectrum. For W 3(OH) and K 3–50A the corresponding frequencies were found to be 250 Ghz and 400 GHz, respectively. The integrated flux was then simply calculated as

$$S_{int} = S_{peak} \cdot \left(1 + \frac{\Theta^2_{source}}{\Theta^2_{beam}}\right) \quad (1)$$

where in the submm regime $\Theta_{source} = 11''$ for W 3(OH) and $\Theta_{source} = 8''$ for K 3–50A.

4. The continuum spectra of the sources

In Figs. 3 and 4 we show the continuum spectra of the observed sources. The straight line is a fit to the data points in the form

$$S_\nu = S_{0_{ff}} \cdot \nu^{-0.1} + S_{0_{D1}} \cdot \nu^{\alpha_1} + S_{0_{D2}} \cdot \nu^{\alpha_2} \quad (2)$$

which reflects the contribution from free-free emission and from two dust-continuum-emission components. The parameters of the spectral fit are given in Table 4 for ν in units of 100 GHz. The observations listed in Table 3 have been put into reasonable bins and are shown as filled dots. The uncertainty of the curves shown in the figure (especially in the short submm-range) can be estimated by comparing the flux densities at a given frequency observed with different resolutions. For both sources such data are available from the JCMT at 384 GHz and in the 860 GHz range, where the published peak flux densities at a given frequency vary by factors of 1.2–1.5 depending on the aperture. After applying the corrections to the peak flux data, the corrected flux densities plotted in Figs. 3 and 4 nearly merge and the differences become comparable or smaller than the internal

Table 4. Fit parameters

Source	$S_{0_{ff}}$	$S_{0_{D1}}$	α_1	$S_{0_{D2}}$	α_2
W 3(OH)	3.151	1.118	2.54	0.00903	5.06
K 3–50A	6.184	0.265	2.60	0.0365	4.01

observational errors. We think that this is a good indicator that the applied procedure works properly.

For a calibration check, it is necessary to get the flux of one of the sources for a given frequency and beam size. This is simply done by calculating the integrated flux of the source using the parameters given in Table 4 and then to scale down the calculated flux according to

$$S_{peak} = S_{int} \cdot \frac{\Theta^2_{beam}}{\Theta^2_{beam} + \Theta^2_{source}} \quad (3)$$

Acknowledgements. Its a pleasure to thank the staff of the 30m telescope for the kind support during the observations. A. Greve, A. Sievers and C. Thum are thanked for encouraging discussions and E. Krügel for careful reading of the manuscript.

References

Altenhoff W.J., Thum C., Wendker H.J., 1994, A&A 281, 161
Chini R., Krügel E., Kreysa E., 1986, A&A 167, 315
Howard E.M., Koerner D.W., Pipher J.L., 1997, ApJ 477, 738
Mauersberger R., Guelin M., Martin-Pintado J., Thum C., Cernicharo J., Hein H., Navarro S., 1989, A&AS 79, 217
Reuter H.-P., Kramer C., Sievers A., Paubert G., Moreno R., Greve A., Leon S., Panis J.F., Ruiz-Moreno M., Ungerechts H., Wild W., 1997, A&AS 122, 271
Sandell G., 1994, MNRAS 271, 75
Ulich B.L., 1981, AJ 86, 1619
Griffin M.J., Ade P., Orton G.S., Robson E.I., Gear W.K., Nolt I.G., Rdostitz J.V., 1986, Icarus 65, 244
Wild W., 1995, "The 30m Manual: A Handbook for the 30m telescope", IRAM preprint No. 377
Wink J.E., Duvert G., Guilleteau S., Güsten R., Walmsley C.M., Wilson T.L., 1994, A&A 281, 505